



# Recent Tomographic Imaging Developments at the PSICHE Beamline

A. King<sup>1</sup> · N. Guignot<sup>1</sup> · J.-P. Deslandes<sup>1</sup> · M. Pelerin<sup>1,2</sup> · I. Joosten<sup>3</sup> · D. De Looff<sup>3</sup> · J. Li<sup>4</sup> · L. Bertrand<sup>1,4</sup> · E. Rosenberg<sup>5</sup> · A. Dewaele<sup>6</sup> · E. Boulard<sup>7</sup> · Y. Le Godec<sup>7</sup> · J.-P. Perrillat<sup>8</sup> · E. Giovenco<sup>8</sup> · G. Morard<sup>7</sup> · T. Weitkamp<sup>1</sup> · M. Scheel<sup>1</sup> · J. Perrin<sup>1</sup> · H. Chevreau<sup>1</sup> · J.-P. Itié<sup>1</sup>

Received: 2 May 2019 / Accepted: 23 September 2019 / Published online: 3 October 2019  
© The Minerals, Metals & Materials Society 2019

## Abstract

PSICHE is a high-energy, multi-technique beamline at the SOLEIL synchrotron facility. It performs X-ray tomography for materials science and other applications and X-ray diffraction for samples at extreme conditions. The beamline has been in service for user experiments since 2013, but is in continual development to add new capabilities. In this article, we present a series of new developments which combine diffraction and tomography and which are of relevance to the study of materials and manufacturing. By combining these techniques, we can add quantitative structural information from diffraction to morphological information obtained by tomography. Recent developments in very fast tomography allow dynamic processes to be studied in situ and in 3D with a time (frequency) resolution of 2 Hz. We have developed in situ sample environments to enable fast tomography measurements at high temperature and pressure, which will allow future studies of industrial processes such as hot isostatic pressing (HIP).

**Keywords** Tomography · Diffraction · Synchrotron radiation · Materials science · Extreme conditions · In situ

## Introduction

PSICHE (pressure, structure, and imaging by contrast at high energy) is the high-energy beamline of the French national synchrotron SOLEIL, located outside Paris [1]. The beamline is designed for two main groups of experiments: Micro-tomography, primarily for materials science

applications, and diffraction for samples at extreme conditions. As such, it is a very flexible instrument, and multiple techniques can be combined in order to provide a more profound understanding of a given system.

## Beamline Characteristics

PSICHE is located on a straight section of the SOLEIL storage ring, with an in-vacuum wiggler insertion device providing a broad-spectrum polychromatic source. Fixed filters remove the lowest X-ray energies, leaving a usable spectrum extending from 17 to 50 keV in monochromatic beam mode, or from 25 to beyond 100 keV in polychromatic mode. With only the permanently installed filters, the white beam flux at the sample position is around  $2 \times 10^{15}$  photons/mm<sup>2</sup>/s. The beam can be monochromated using a double-crystal Si (111) in Bragg–Bragg geometry. In monochromatic mode, the photon flux is around  $3 \times 10^{11}$  photons/mm<sup>2</sup>/s at 25 keV. In both modes, a bendable mirror can be used to focus or condense the beam vertically to increase flux density [1].

✉ A. King  
king@synchrotron-soleil.fr

<sup>1</sup> Synchrotron SOLEIL, BP 38, Saint-Aubin, Gif-sur-Yvette, France

<sup>2</sup> MINES ParisTech, PSL University, Centre des Matériaux UMR CNRS 7633, BP 87, 91003 Évry, France

<sup>3</sup> Cultural Heritage Agency of the Netherlands RCE, Amsterdam, The Netherlands

<sup>4</sup> IPANEMA, CNRS, ministère de la Culture, UVSQ, USR 3461, Université Paris–Saclay, 91192 Gif-sur-Yvette, France

<sup>5</sup> IFP Energies Nouvelles, Rueil-Malmaison, France

<sup>6</sup> CEA, DAM, DIF, Arpajon, France

<sup>7</sup> IMPMC, UMR 7590 - Sorbonne Université/CNRS/MNHN/IRD, 75005 Paris, France

<sup>8</sup> Laboratoire de Géologie de Lyon, UMR 5276 CNRS, ENS Lyon – Université Lyon 1, Villeurbanne Cedex, France

## Diffraction

Diffraction can be performed in both energy-dispersive and angular-dispersive modes. In angular-dispersive mode, the monochromator is used to select the beam energy. Diffraction from the sample is measured using 2D area detectors. In energy-dispersive mode, a polychromatic incident beam is defined using slits. Additional filters may be added to reduce the incident flux on the sample. Two sets of slits, positioned after the sample in the horizontal plane, define the diffracted beam angle. A rotation system allows the diffraction angle to be varied between  $-5^\circ$  and  $+30^\circ$  ( $2\theta$ ) [2]. An energy-sensitive germanium detector is used to detect the diffracted spectrum. An advantage of the latter approach is that because both the incident and diffracted beams are collimated by slits, the signal is detected from a well-defined gauge volume in space (Fig. 1). This 3D spatial resolution makes energy-dispersive diffraction a natural complement to 3D tomographic imaging techniques, and the use of a polychromatic beam can be easily combined with fast tomography measurements using filtered white beam. However, the alignment of the diffraction measurement with the tomography measurement must be assured.

## Tomography

Tomography experiments can also be performed in monochromatic or polychromatic modes according to the

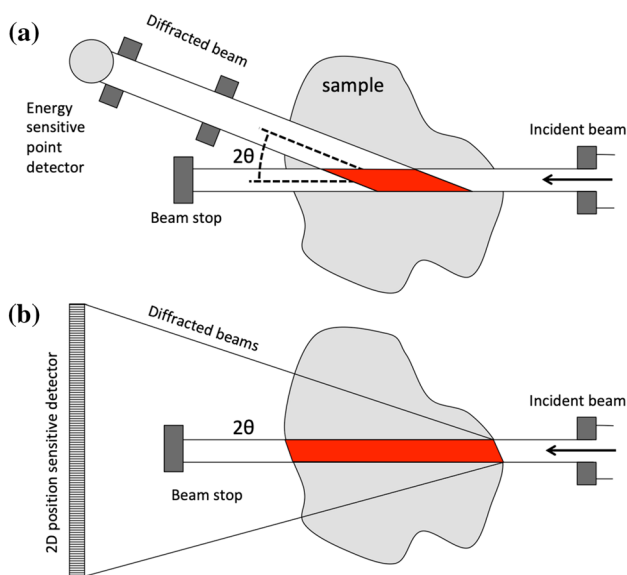


**Fig. 1** **a** Energy-dispersive diffraction geometry. The diffraction and fluorescence signal comes from the zone defined by the intersection of the incident and diffracted beams (in red). **b** Angular-dispersive diffraction geometry. Note that in both cases sample–detector distances are much greater than the sample or diffracting volume size

requirements of the experiment. Monochromatic beam mode is used for applications that do not require very high beam intensities, for samples requiring the lowest beam energies, or to be as quantitative as possible in determining attenuation coefficients [3]. It is also used for experiments combining tomography with angular-dispersive diffraction. It can also be used to exploit anomalous contrast due to X-ray absorption edges. In polychromatic beam mode, various filtering strategies are used to define the beam spectrum in order to adapt the flux and the average photon energy to the experimental requirements. More attenuating samples (larger cross section or more dense) require higher photon energies, and faster tomography for time resolution requires higher flux. Notably, an X-ray mirror is used as an adjustable low-pass energy filter, and filters exploiting X-ray absorption edges are used as energy-selective filters (notably silver, tin, and tungsten). In this way, the average beam energy can be varied between 25 and 100 keV, whilst maintaining a band-pass sufficiently narrow to avoid band-hardening artefacts (typically  $\Delta E/E \sim 10^{-1}$ , versus  $\sim 10^{-4}$  for a crystal monochromator). Such filtered white beam for imaging is generally referred to as “pink beam” [1, 3, 4].

## Combining Tomography and Diffraction

Recent experiments performed at PSICHE have developed different combinations of tomography and diffraction. These have, broadly, followed two different approaches. The principal approach uses polychromatic beam for imaging and energy-dispersive diffraction and will be described in detail below. Other experiments have been performed in monochromatic mode, using angular-dispersive diffraction. The construction of the PSICHE beamline does not allow pink-beam imaging to be easily combined with monochromatic diffraction, or vice versa, but this is not the case for all beamlines (e.g. the DIAD beamline under construction at Diamond Light Source, UK). The approaches differ in the acquisition time required, and in the spatial resolution and reciprocal space coverage of the diffraction measurement. Typically, tomographic acquisition is faster with polychromatic illumination because of the higher flux. Energy-dispersive diffraction offers 3D spatial resolution within a sample (Fig. 1), whilst angular-dispersive diffraction is spatially resolved in only two directions, unless conical or spiral slit systems are employed [5, 6], or tomographic reconstruction techniques are used [7]. Energy-dispersive diffraction typically covers a smaller region of reciprocal space than angular-dispersive diffraction with a 2D detector and currently requires a longer acquisition time due to the maximum count rate of the detector. The instrumental broadening of diffraction peaks is also larger for energy-dispersive diffraction. The most suitable combination of techniques will depend

on the requirements of the measurement. In both cases, the eventual aim is to provide a fuller description of a given sample, as is commonly performed in electron microscopy, where imaging is combined with diffraction or fluorescence modes in a user-friendly manner [8]. Diffraction adds information not available from the absorption or phase contrast tomography, such as the crystallographic phase identification or elastic strain measurement. During experiments at high pressure, the shift of diffraction peaks is typically used to measure pressure and temperature via equations of state. The energy-sensitive detector can also detect X-ray fluorescence, adding further compositional information.

Planned upgrades to the energy-dispersive diffraction system at PSICHE will add a new seven-element germanium detector, together with state-of-the-art readout electronics. These improvements will allow much faster acquisitions, reaching the speed of 2D detectors, and improve the efficiency of the system so that the radiation dose received by the sample is reduced.

### Setup, Alignment, and Acquisition Protocol

The tomography and diffraction techniques used are both well established. However, combining the measurements in an efficient and easy-to-use way requires the development of a clearly defined measurement protocol and software routines. Here, we describe the procedure in which tomography is performed using pink-beam illumination, and diffraction is performed in white beam, energy-dispersive mode. Changing between imaging and diffraction modes requires only that the filters be removed from the beam that slits in front of the sample are closed to define the beam for diffraction, and that the tomography detector is translated out of the beam and is completely automated.

The coordinate systems of the tomograph and the diffraction instrument are aligned. The tomograph is first aligned as normal (rotation axis perpendicular to the beam and parallel to the columns of the camera and rotation axis centred with respect to the camera). We then ensure that the slits are aligned with the rotation axis and the centre of the camera field of view. Finally, a foil is placed on the centre of rotation using the imaging camera. The diffraction or fluorescence signal from this foil is used to bring the gauge volume of the diffraction detector to the rotation axis position. The diffraction angle is calibrated using a standard material.

Thus aligned, a tomography reconstruction can be used to guide the diffraction measurement. The rotation axis position is well defined in the reconstructed volume (usually centred). The sample alignment motor positions and the reconstructed voxel size are automatically saved with the data. With this information, a given voxel position in the reconstruction can be selected and used to generate a set of motor positions that will bring that point in the sample to the

centre of rotation and hence the diffraction gauge volume. Because the gauge volume is aligned with the rotation axis, a polycrystalline sample can be oscillated during diffraction to increase the number of grains sampled. A 1D or 2D grid of points can be defined within a reconstruction and used to generate a beamline control script for automatic measurement by diffraction. This allows the relatively slow diffraction measurement to be used efficiently. All these steps are handled interactively via Python functions which interface with the Python-based beamline control software.

### Typical Results

Figure 2 shows how such a measurement was applied to study the 3D composition of an archaeological specimen. The sample is a fragment of ancient textile material that has been “mineralised” during corrosion of an adjacent metallic object, similar to that described by Li et al. [3]. The sample was first imaged using pink-beam tomography (Fig. 2a). This was a fast, low-quality scan for alignment purposes. Figure 2b shows a chosen section through the reconstructed volume. A grid of 400 points (a  $20 \times 20$  array, covering  $\sim 2.3 \times 2.3 \text{ mm}^2$ ) was defined around a region of

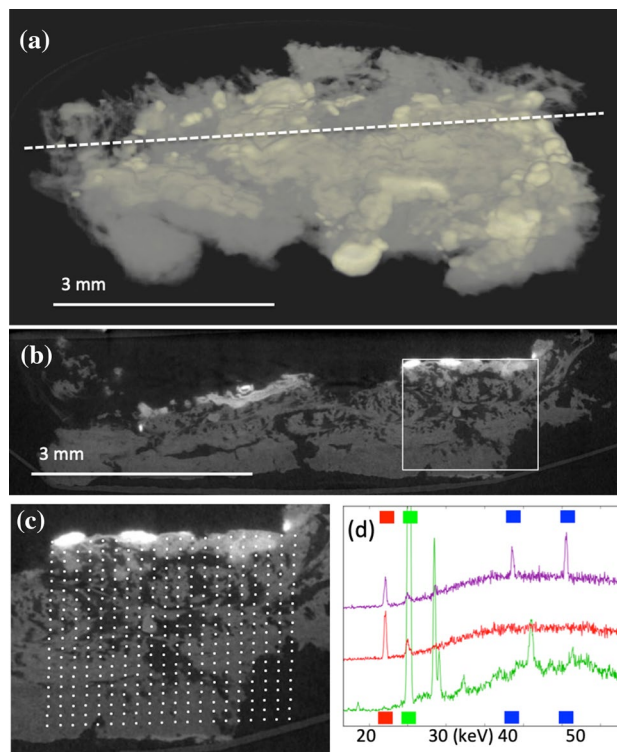


**Fig. 2** Energy-dispersive diffraction mapping. **a** Tomogram of the mineralised archaeological textile sample. **b** Section through the reconstruction, **c** grid of measurement points defined on the section. **d** Examples of energy-dispersive spectra acquired at each point. The colour mark peaks used in this example: red: silver fluo., green: tin fluo., blue: quartz diffraction

interest (Fig. 3). Diffraction and fluorescence spectra were acquired at each point. The sample was rotated through  $360^\circ$  during 30 s counting time. Figure 2d shows part of some of the spectra, including two fluorescence peaks (silver and tin  $K\alpha$ ) and two diffraction peaks assigned to quartz. The intensity of different diffraction or fluorescence peaks can be extracted and overlaid on the tomography data. In this example, single peaks were selected and fitted with a Gaussian profile to extract the intensity above background. Figure 3 shows the results of mapping. The peak intensities were normalised by the maximum values and assigned to the red, green, and blue channels to represent the local composition. The resulting images reveal the spatial distributions of silver and tin species in the artefact, and the presence of a quartz particle (from the sandy soil) that has a similar attenuation coefficient to the surrounding material.

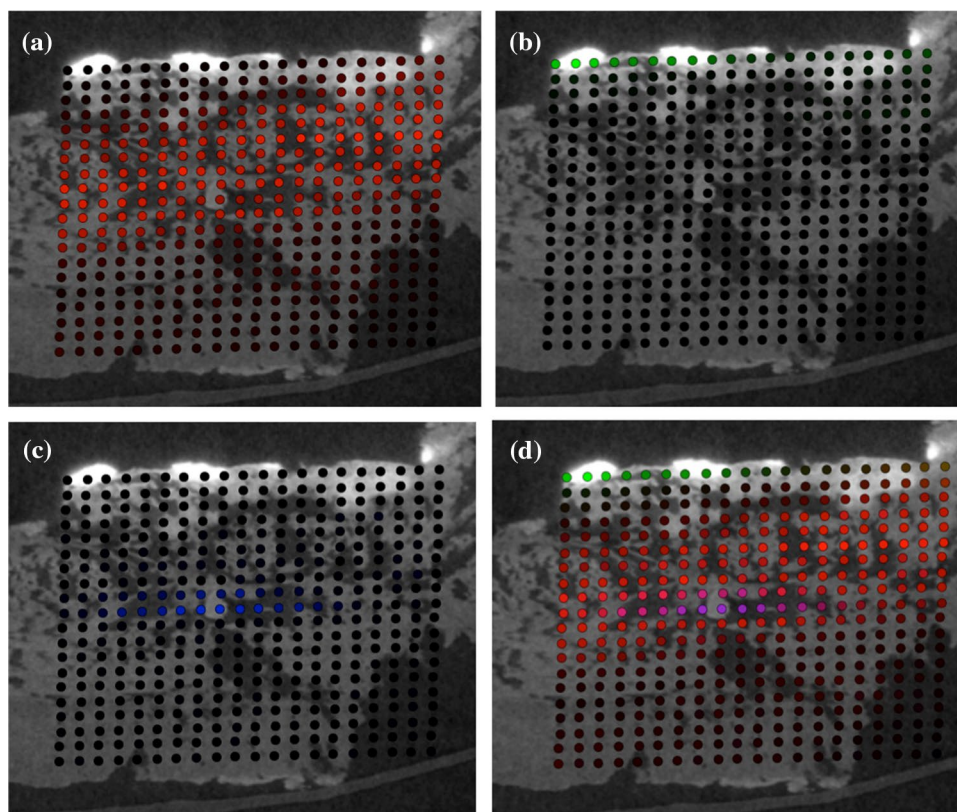
### Fast Tomography

Fast tomography (0.5–10 s per tomogram, or faster) is needed to study dynamic processes with short characteristic timescales (from tens of seconds to minutes) such as damage propagation, phase transitions, or liquid percolation [9]. It is also essential for studying phenomena that cannot be interrupted without changing the behaviour. An

example would be in situ mechanical testing of polymer matrix composites, which exhibit significantly different mechanical behaviours during continuous traction or interrupted traction. Recent experiments at PSICHE have exploited the high flux available in pink-beam mode to perform fast tomography or radiography. With only the permanently mounted filters in place, the available photon flux is of the order of  $2.6 \times 10^{15}$  photons  $s^{-1} mm^{-2}$  during 500 mA operation, with an average energy of around 30 keV. In practice, some filtering is usually necessary to protect the sample and detector. The very high flux, as well as initial feasibility tests, indicates that single-bunch imaging [10] is feasible at PSICHE.

For initial fast tomography experiments, a PCO Dimax HS4 camera [11] has been used on loan from the ANATOMIX beamline [12]. This camera is capable of recording more than 2000 full frames per second. The maximum speed of the Leuven RT500 rotation stage as configured is greater than  $360^\circ/s$ . Therefore, it is a feasible to acquire a full resolution tomogram (1500 projections recorded over  $180^\circ$  rotation) in 0.5 s, even with a large sample environment for in situ measurements. Figure 4 shows a section from  $2000^3$  voxel volume, reconstructed from 1500 projections recorded in 1.5 s with a voxel size of 1.1 microns. The pink-beam energy was around 25 keV, with a photon flux of  $\sim 9 \times 10^{13}$  photons  $s^{-1} mm^{-2}$ .

**Fig. 3** Energy-dispersive diffraction mapping results. **a** Silver fluorescence, **b** tin fluorescence, **c** quartz diffraction, and **d** combined results



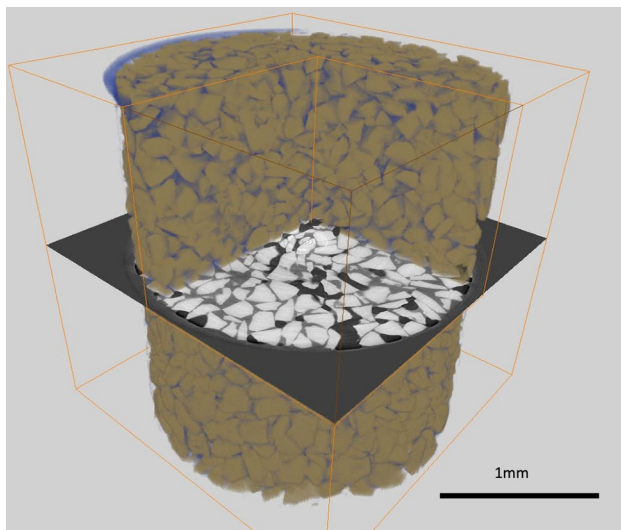


**Fig. 4** Tomogram acquired in 1.5 s, showing sand, water, and a liquid phase. Sample diameter 2 mm, voxel size 1.1 microns

### High Heat Load Scintillator Support

These experiments have suggested that one limiting factor in acquisition speed is the heat load on the scintillator (typically cerium-doped lutetium aluminium garnet, LuAG:Ce). Heat causes the thin scintillator to deform, which can result

in a blurred image as the scintillator moves out of the depth of field of the microscope objective. This was the case for the example as shown in Fig. 4. Further increasing the heat load will cause the scintillator to fracture. We have started trials of a scintillator support designed to give better mechanical support and to improve heat transfer out of the scintillator. Currently, scintillators are mounted over a hole in an aluminium plate using Kapton tape, in such a way that there is little surface contact and hence poor heat transfer by conduction from the scintillator. It should be noted that LuAG is a poor thermal conductor ( $7\text{--}10\text{ Wm}^{-1}\text{ K}^{-1}$ , compared with aluminium  $235\text{ Wm}^{-1}\text{ K}^{-1}$  or graphite  $25\text{--}470\text{ Wm}^{-1}\text{ K}^{-1}$ ). In the new design, the scintillator is held in a sandwich arrangement between a graphite plate and an aluminium piece as shown in Fig. 5. Graphite is used for its low attenuation of X-rays and relatively good thermal conductivity. CVD diamond has a better thermal conductivity, but typically fluoresces when exposed to the X-ray beam, producing unwanted light. Aluminium is used for its good thermal conductivity. This type of sandwich structure is used with success for beam filters, which must absorb significant power from the beam. In particular, it allows filtering with low melting point filters such as tin which would otherwise melt. The key parameter is to minimise the diffusion distance for heat transfer. In such a sandwich structure, the majority of the heat load is deposited in the scintillator, because it is necessarily highly attenuating of the X-ray beam. Rather

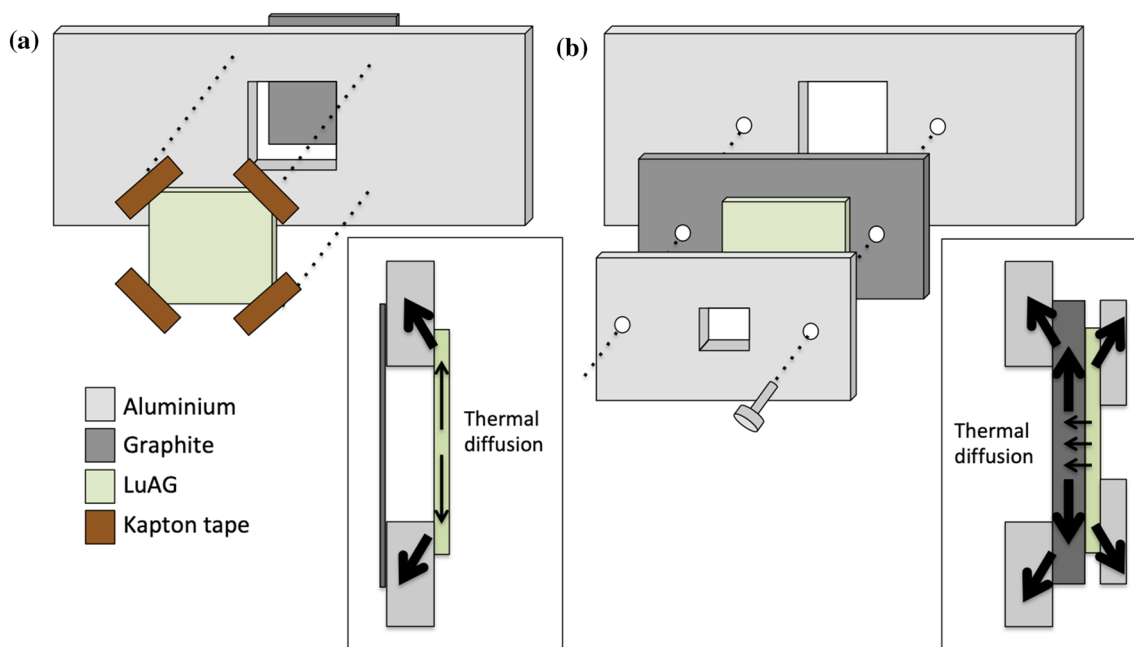


**Fig. 5** Managing heat load in scintillators **a** standard scintillator support. Heat from the beam is conducted out through the scintillator, with poor thermal contact to the aluminium support (shown schematically by arrows on the cross section). A thin piece of vitreous carbon

is a barrier to visible light. **b** High heat load design. Heat is transferred directly to thick graphite and aluminium plates and conducted through the plates to the support. The scintillator is held mechanically between the plates to avoid deformation

than diffusing out through the scintillator, the heat can diffuse to the adjacent sandwich material, reducing the diffusion distance from the lateral dimension of the scintillator to the thickness of the scintillator, typically a difference of two orders of magnitude, from millimetres to tens of microns. This is shown schematically in Fig. 5. Simple one-dimensional diffusion calculations suggest that the temperature of a LuAG scintillator can be reduced by many hundreds of degrees, avoiding deformation and allowing much higher flux to be used without risk of scintillator damage.

## Fast Tomography at Extreme Conditions

In recent years, tomography has become an increasingly important diagnostic tool in high-pressure research [13, 14]. Two main types of experiment have been developed. The first is the use of panoramic diamond anvil cells with X-ray transparent gaskets [15, 16]. Diamond anvil cells (DAC) can reach very high pressures ( $> 100$  s GPa), and panoramic cell designs allow projections to be recorded over to  $\sim 150^\circ$ . High temperatures could in principle be reached using laser or resistive heating, but significantly complicate the experimental design [15]. The principle limitation of the DAC is the very small sample size, typically in the range of tens of microns. This means that X-ray microscopy techniques are required for tomography, complicating the experiment and requiring long data acquisition times, from tens of minutes to hours per tomogram [16]. The second approach uses large volume cells (Paris–Edinburgh [17] or Drickamer cells [18]) compressed between two opposed anvils that can rotate inside a load frame. This means that projection data can be recorded over a full  $180^\circ$  angular range. Sample sizes are in the order of one millimetre and are thus compatible with parallel-beam tomography. However, the significant mechanical challenge of rotating the anvils under load means that rotation speeds are limited, and hence, the acquisition of a tomogram requires at least tens of minutes. In recent years, the use of fast parallel-beam tomography at synchrotron sources has become widespread (see Maire and Withers' review [9], and "Fast Tomography" section of the current paper). Long acquisition times are a severe limitation for in situ studies of dynamic phenomena. To avoid motion artefacts, the acquisition time must be short enough that the sample does not evolve significantly during the acquisition. This is particularly difficult for samples at high temperatures and pressures, and especially for samples containing liquid phases.

In order to perform fast, in situ tomography at high pressures and temperatures, we have developed a new Paris–Edinburgh press optimised for tomography [19]. This is known as the UToPEC (Ultra-fast Tomography Paris–Edinburgh Press) (Fig. 6a). The press is based on the

VX panoramic Paris–Edinburgh design. Urakawa et al. [20] describe a press with a similar design, but without developing the high-speed tomography application. The geometry has been optimised for parallel-beam imaging with a pixel size of  $1.3 \mu\text{m}$ , corresponding to a spatial resolution of  $> 2.6 \mu\text{m}$  given the Nyquist–Shannon criterion [21]. The angular opening of the press has been increased to  $165^\circ$ , which allows good reconstructions to be obtained using standard filtered backprojection techniques. The external diameter of the press has been minimised in order that the sample to detector distance can be less than 90 mm. This is necessary in order to achieve a spatial resolution of  $\sim 3$  microns in the hutch at PSICHE due to source size blurring ( $\sim 900 \mu\text{m}$  full width at half maximum horizontal source size at 24 m source to sample distance [private communication. T. Moreno, SOLEIL]), with the constraints imposed by phase contrast effects at energies below 30 keV [22]. To enable fast tomography with continuous rotation, all connections to the press (electricity for resistive heating of the sample assembly, water for cooling, electrical connections for alignment motors) pass through rotary couplings. The only exception is the hydraulic oil connection for pressurising the sample assembly. During an experiment, the sample is first compressed to the target pressure. A valve is then closed, and the high-pressure oil pump is disconnected. The press is then able to rotate continuously, allowing fast tomography as described in "Fast Tomography" section. Tomography can be performed with  $1.3 \mu\text{m}$  pixel size ( $\sim 3$ – $5$  micron true resolution), with minimal reconstruction artefacts, at high pressures and temperatures (up to 10 GPa and 2000C) and with less than one second per complete tomogram. Figure 6 presents some typical recent results. Figure 6b shows an iron microstructure close to the  $\alpha$ – $\gamma$ – $\epsilon$  triple point of the iron phase diagram at ( $\sim 10$  GPa and 510C,  $1.3 \mu\text{m}$  voxel size, 60 s per tomogram). Figure 6c shows a measurement of the percolation of barium carbonate (liquid) through natural olivine grains ( $\sim 29$  keV,  $2.2 \mu\text{m}$  voxel size, 1 s per tomogram). Figure 6d shows the evolution of porosity in an additively manufactured aluminium sample during hot isostatic pressing ( $\sim 50$  keV,  $1.3 \mu\text{m}$  voxel size, 90 s per tomogram). In both cases, the dynamic processes in the sample have proved difficult to image with longer acquisition times as changes in the sample during acquisition cause artefacts in the reconstruction. The press is of course compatible with X-ray diffraction, which is used for the measurement of pressure and temperature using calibrant materials with well-known equations of state. It is equally possible to apply the diffraction mapping techniques presented in "Combining Tomography and Diffraction" section. We anticipate that this system will be of interest not only for geophysical applications, but also for materials science and materials processing studies of applications such as hot isostatic pressing.

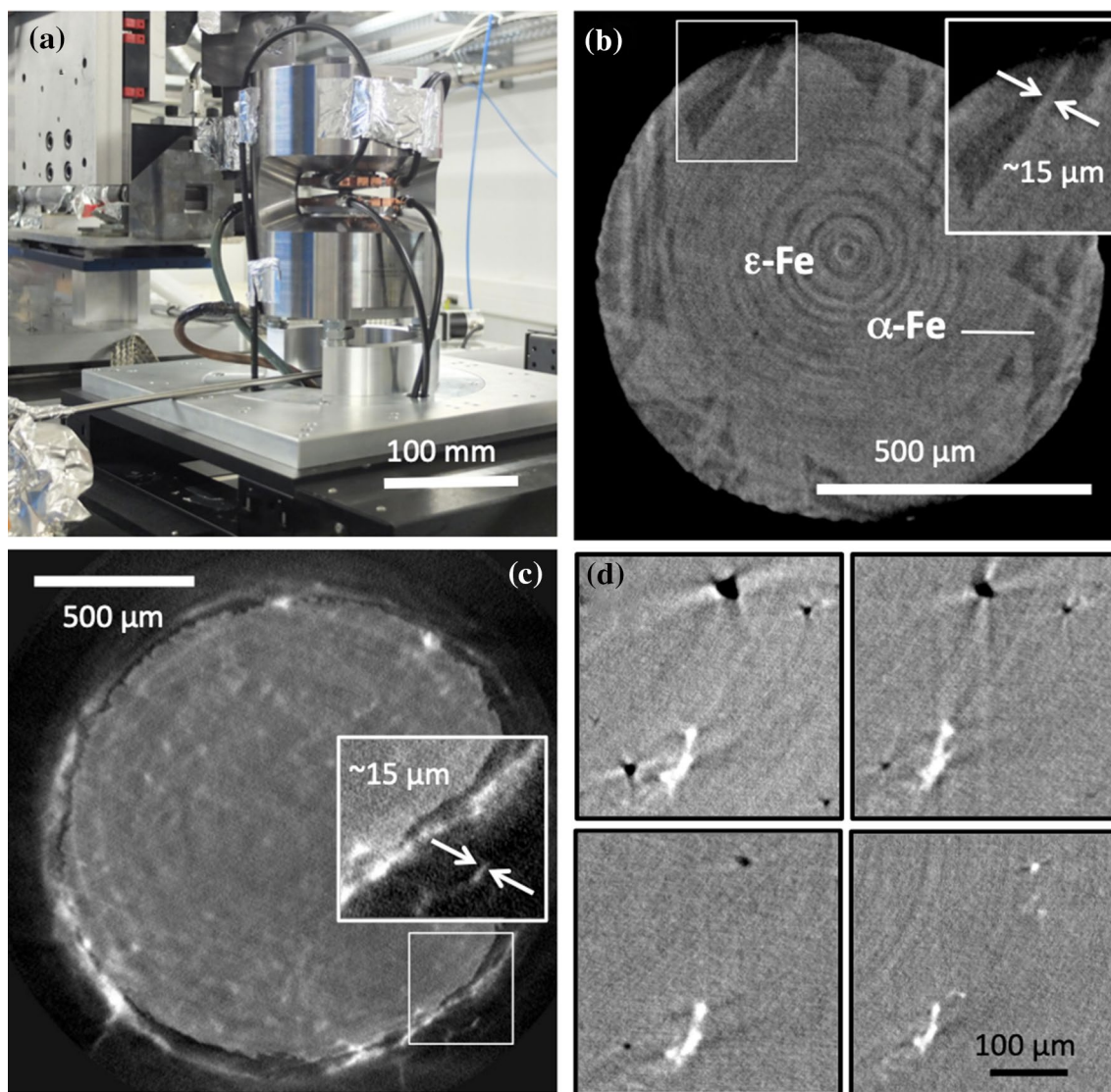


**Fig. 6** **a** UToPEC press for fast tomography at high temperature and pressure. **b** Section through an iron sample showing the  $\alpha$ - $\epsilon$  phase transition in iron at 10 GPa and 510C, and **c** section through of natural olivine (solid, grey) and barium carbonate (liquid, white). Tomo-

gram acquired in one second, 2.2 micron voxel size. **d** Evolution of porosity in a sub-volume of an aluminium sample during hot isostatic pressing (from top-left, RTP, RT  $\sim$  100 MPa, 300C  $\sim$  100 MPa, 380C  $\sim$  100 MPa)

## Conclusions

This article presents three examples of recent progress in imaging experiments at the PSICHE beamline. These represent the ongoing effort to enlarge the range of measurements that are possible and to develop combinations of tomography and diffraction techniques to better serve the scientific and industrial user community. The combination of techniques can bring particular benefits to in situ materials science and high-pressure research, reflecting the interests of the beamline.

**Acknowledgements** The Dimax camera was on loan from the beamline ANATOMIX, an Equipment of Excellence (EQUIPEX) funded by the Investments for the Future program of the French National Research Agency (ANR), Project NanoimagesX, Grant No. ANR-11-EQPX-0031.

## Compliance with Ethical Standards

**Conflict of interest** The authors declare that they have no conflict of interest.

## References

1. King A, Guignot N, Zerbino P, Boulard E, Desjardins K et al (2016) Tomography and imaging at the PSICHE beamline of the SOLEIL synchrotron. *Rev Sci Instrum* 87:093704. <https://doi.org/10.1063/1.4961365>
2. Wang Y, Uchida T, Von Dreele R, Rivers ML, Nishiyama N, Funakoshi K, Nozawa A, Keneko H (2004) A new technique for angle-dispersive powder diffraction using an energy-dispersive setup and synchrotron radiation. *J Appl Crystallogr* 37:947–956
3. Li J, Guériau P, Bellato M, King A, Robbiola L, Thoury M, Bailon M, Fossé C, Cohen SX, Moulhéat C, Thomas A, Galtier P, Bertrand L (2019) Synchrotron-based phase mapping in corroded metals: insights from early copper-base artifacts. *Anal Chem* 91(3):1815–1825. <https://doi.org/10.1021/acs.analchem.8b02744>
4. Rivers M (2017) High-speed tomography using pink beam at GeoSoilEnviroCARS. In: Conference: SPIE optical engineering + applications, United States. <https://doi.org/10.1117/12.2238240>
5. Nielsen SF, Wolf A, Poulsen HF, Ohler M, Lienert U, Owen RA (2000) A conical slit for three-dimensional XRD mapping. *J Synchrotron Radiat* 7:103–109. <https://doi.org/10.1107/S090904950000625>
6. Martins RV, Honkimäki V (2003) Depth resolved strain and phase mapping of dissimilar friction stir welds using high energy synchrotron radiation. *Texture Microstruct* 35:145–152. <https://doi.org/10.1080/07303300310001628625>
7. Bleuët P, Welcomme E, Dooryhée E, Susini J et al (2008) Probing the structure of heterogeneous diluted materials by diffraction tomography. *Nat Mater* 7:468–472. <https://doi.org/10.1038/nmat2168>
8. Goldstein JI, Newbury DE, Michael JR, Ritchie NWM, Scott JHJ, Joy DC (2018) Scanning electron microscopy and X-ray microanalysis. Springer, New York. <https://doi.org/10.1007/978-1-4939-6676-9>
9. Maire E, Withers PJ (2014) Quantitative X-ray tomography. *Int Mater Rev* 59(1):1–43
10. Rack A, Scheel M, Hardy L, Curfs C, Bonnin A, Reichart H (2014) Exploiting coherence for real-time studies by single bunch imaging. *J Synchrotron Radiat* 21:815–818. <https://doi.org/10.1107/S1600577514005852>
11. pco.dimax HS4. PCO AG, Germany. <https://www.pco.de/highspeed-cameras/pcodimax-hs4/>. Accessed 29 April 2019
12. Weitkamp T, Scheel M, Giorgetta JL, Joyet V, Le Roux V, Cauchon G, Moreno T, Polack F, Samama JP (2017) The tomography beamline ANATOMIX at Synchrotron SOLEIL. In: IOP conference series: journal of physics conference series, vol 849, p 012037. <https://doi.org/10.1088/1742-6596/849/1/012037>
13. Cnudde V, Boone MN (2013) High-resolution X-ray computed tomography in geosciences: a review of the current technology and applications. *Eath Sci Rev* 123:1–17. <https://doi.org/10.1016/j.earscirev.2013.04.003>
14. Fusses F, Xiao X, Schrank C, De Carlo F (2014) A brief guide to synchrotron radiation-based microtomography in (structural) geology and rock mechanics. *J Struct Geol* 65:1–16. <https://doi.org/10.1016/j.jsg.2014.02.005>
15. Mao WL, Lin Y, Liu Y, Liu J (2019) Applications for nanoscale imaging at high pressure. *Engineering*. <https://doi.org/10.1016/j.eng.2019.01.006>
16. Lin Y, Zeng Q, Yang W, Mao WL (2013) Pressure-induced densification in GeO<sub>2</sub> glass: a transmission x-ray microscopy study. *Appl Phys Lett* 103:261909. <https://doi.org/10.1063/1.4860993>
17. Philippe J, Le Godec Y, Mezouar M, Berg M et al (2016) Rotating tomography Paris–Edinburgh cell: a novel portable press for micro-tomographic 4-D imaging at extreme pressure/temperature/stress conditions. *High Press Res*. <https://doi.org/10.1080/08957959.2016.1221951>
18. Wang Y, Uchida T, Westferro F, Rivers ML et al (2005) High-pressure X-ray tomography microscope: synchrotron computed microtomography at high pressure and temperature. *Rev Sci Instrum* 76:073709–1–073709–6. <https://doi.org/10.1063/1.1979477>
19. Boulard E, King A, Guignot N, Deslandes J-P et al (2018) High-speed tomography under extreme conditions at the PSICHE beamline of the SOLEIL Synchrotron. *J Synchrotron Radiat* 25:818–825. <https://doi.org/10.1107/S1600577518004861>
20. Urakawa S, Terasaki HP, Funakoshi K, Uesugi K, Yamamoto S (2010) Development of high pressure apparatus for X-ray microtomography at SPring-8. *J Phys Conf Ser* 215:012026. <https://doi.org/10.1088/1742-6596/215/1/012026>
21. Kak AC, Slaney M (1988) Principles of computerized tomographic imaging. IEEE Press
22. Weitkamp T, Haas D, Wegrzynek D, Rack A (2011) ANKAphase: software for single-distance phase retrieval from inline X-ray phase-contrast radiographs. *J Synchrotron Radiat* 18:617–629. <https://doi.org/10.1107/S0909049511002895>